Journal of Photochemistry & Photobiology, A: Chemistry 483 (2027) 117661

Contents lists available at ScienceDirect

Journal of Photochemistry & Photobiology, A: Chemistry

journal homepage: www.elsevier.com/locate/jphotochem

Enhanced photodynamic antimicrobial approach: carboxylated porphyrins as potent light-activated photosensitizers to reduce effectively viability of *Staphylococcus aureus* and *Escherichia coli*

Leandro M.O. Lourenço [a,*], Cátia Vieira [b], Duarte Rosa [b], Maria Bartolomeu [b,c], Adelaide Almeida [b,*]

[a] LAQV-REQUIMTE and Department of Chemistry, University of Aveiro, 3810–193 Aveiro, Portugal
[b] CESAM and Department of Biology, University of Aveiro, 3810–193 Aveiro, Portugal
[c] Centre for Interdisciplinary Research in Health (CIIS), Universidade Católica Portuguesa, Faculty of Dental Medicine, 3504–505 Viseu, Portugal

ARTICLE INFO

Keywords:
Carboxylated porphyrins
Antimicrobial photoinactivation (PDI)
S. aureus bacteria
E. coli bacteria
Reactive oxygen species (ROS)
Reactive iodide species (RIS)

ABSTRACT

Antimicrobial photoinactivation (PDI) is an emerging therapeutic strategy capable of efficiently eliminating a wide range of microorganisms. An important advantage of this approach is the absence of resistance development, making PDI a promising alternative for infection control. In this study, tetra-substituted free-base porphyrins (H_2Pors **1**–**3**) bearing thiocarboxylic acid groups were synthesized, characterized, and evaluated for the first time as photosensitizers in the PDI of *Staphylococcus aureus* and *Escherichia coli*. The compounds were tested at low concentrations (1.0 μM for *S. aureus* and 10.0 μM for *E. coli*), under white light irradiation, both in the absence and presence of potassium iodide (KI, 100 mM). All porphyrins exhibited strong antibacterial activity against *S. aureus*, achieving inactivation to the detection limit within 10–30 min, with H_2Por **2** showing the highest efficacy. In contrast, the porphyrins alone were not effective against *E. coli*. However, when combined with KI, bacterial inactivation to the detection limit of the method was achieved. Additionally, KI significantly reduced the treatment time required for *S. aureus* inactivation. Overall, H_2Pors **1**–**3**+KI demonstrate strong potential as photosensitizers for effective PDI, highlighting their potential applicability in biological settings.

1. Introduction

The overuse and misuse of antibiotics have driven the rise of multiple drug-resistant (MDR) bacteria [1]. This growing problem presents a significant challenge, as infections caused by these resistant strains lead to severe health conditions and often require the use of last-resort antibiotics, which can be potentially harmful. However, many bacterial strains have already developed resistance to these very antibiotics [1,2]. Relying solely on the development of new antibiotics is not a sustainable solution, as they too will inevitably lose their effectiveness over time [3]. Therefore, there is an urgent need to explore and develop alternative therapeutic strategies.

Photoinactivation (PDI) of microorganisms offers a promising alternative to traditional antibiotic treatments. PDI harnesses the combined power of a photosensitizer (PS), molecular oxygen (O_2), and light to generate cytotoxic reactive oxygen species (ROS) such as singlet oxygen ($^1O_2$), superoxide anion ($O_2^{\bullet-}$), hydroxyl radicals ($OH^{\bullet}$), and hydrogen peroxide (H_2O_2) [4–6]. These ROS cause widespread, nonspecific damage to the bacterial cell wall, cytoplasmic membrane, intracellular proteins, and deoxyribonucleic acid (DNA). As a result, the development of resistance to PDI seems highly unlikely, and no such resistance has been documented to date [7].

Macrocyclic dyes such as porphyrin (Por) derivatives [8,9], and other related compounds such as chlorins [8,10,11] and phthalocyanines [5,12,13], have been employed as versatile molecules for the microbial PDI treatment. While neutral and anionic photosensitizers are effective at eradicating Gram-positive bacteria, their activity against Gram-negative bacteria is limited due to the reduced sensitivity of these organisms to the photodynamic treatment [4,11,12,14–16]. In Gram-negative bacteria, the outer membrane acts as an additional barrier, obstructing the interaction between the PS and ROS-sensitive molecules [17]. Despite these facts, the tetrapyrrolic macrocycles have been structurally modified with peripheral functional groups [18,19], including carboxylic [20], hydroxyl [21], and charged groups [22],

* Corresponding authors.
E-mail addresses: leandrolourenco@ua.pt (L.M.O. Lourenço), aalmeida@ua.pt (A. Almeida).

https://doi.org/10.1016/j.jphotochem.2026.117661
Received 6 May 2026; Received in revised form 1 July 2026; Accepted 30 August 2026
Available online 31 August 2026

promoting better solubility and amphiphilicity of these molecules for several treatments in biological targets [21,22]. In this way, recent studies on photodynamic antimicrobial strategies, food preservation, antimicrobial films/coatings, and light-activated microbial control have been developed [23–29].

Recent research has shown that inorganic salts such as sodium thiocyanate [30], sodium azide [31], sodium bromide [32], and potassium iodide (KI) [11,12,31,33] can significantly enhance the PS effectiveness against both Gram-positive and Gram-negative bacteria [34]. Specifically, the addition of KI has been found to boost the activity of neutral, negatively charged, and positively charged PSs against *Staphylococcus aureus* (Gram-positive bacterium) and *Escherichia coli* (Gram-negative bacterium) [11,12,31,35]. The enhanced efficacy of KI is attributed to the rapid production of highly toxic and reactive iodine species (RIS, Fig. 1). Studies suggest that the potentiation effect of KI occurs through a series of parallel reactions, beginning with the interaction of $^1O_2$ with iodide (I^-), which leads to the formation of peroxyiodide ($HOOI_2^-$) [11]. This intermediate can then proceed down two possible pathways: one producing H_2O_2 and free iodine (I_2/I_3^-), or the other resulting in the homolytic cleavage of peroxyiodide to form the iodide radical anion ($I_2^{-\bullet}$) [33]. If H_2O_2 and I_2/I_3^- are primarily responsible for bacterial inactivation, the PDI curve exhibits a sharp inactivation profile. On the other hand, if the $I_2^{-\bullet}$ dominates, the killing curve progresses more gradually [36].

The chemical structure of a PS is crucial in determining its physicochemical and biological properties [37,38]. By introducing peripheral substituents, specific functionalities can be tailored, such as enhancing solubility and increasing $^1O_2$ quantum yield [39]. Therefore, multifluorinated tetrapyrrolic macrocycles have been modified with thioglycolic, 3-mercaptopropionic, or mercaptosuccinic acid units [40]. Porphyrins bearing carboxylic groups have been investigated as promising antimicrobial agents against bacteria and fungi with interesting results of microbial inactivation [20,41].

In light of our pursuit of efficient PSs for the PDI of microorganisms, this study evaluated for the first time the efficiency of tetra-substituted thiocarboxylic acid porphyrins (H_2Pors **1**–**3**, Scheme 1) for the PDI process of *Staphylococcus aureus* and *Escherichia coli*, representing Gram-positive and Gram-negative bacterial models, to determine their potential for clinical photodynamic treatments and environmental applications. In this context, H_2Pors **1** and **2** [40] were synthesized containing four carboxylic groups and a new compound of H_2Por **3** featuring eight (Scheme 1). The PDI experiments of *S. aureus* and *E. coli* bacteria were conducted using these PSs **1**–**3** varying their concentrations (5.0 and 10.0 μM), both with and without the addition of KI (100 mM), under white light irradiation (400–700 nm) at irradiance 50 mW.cm^{-2}.

2. Materials and methods

2.1. General experimental procedures

H_2Pors **1** and **2** were previously synthesized and reported [40], whereas H_2Por **3** was prepared for the first time in the present study. All reagents used in this study were obtained from Merck and used without further purification due to their high purity. Solvents were distilled and dried following established literature procedures [42]. Analytical thin-layer chromatography (TLC) was performed on precoated silica sheets with silica gel (Merck 60, 0.2 mm thick). Column chromatography was conducted using silica gel (Merck, 35–70 mesh).

The ^{1}H and ^{19}F nuclear magnetic resonance (NMR) spectra were recorded on a Bruker AMX 300 spectrometer at 300.13 MHz and 282.38 MHz, respectively, while the ^{13}C NMR spectra were obtained using a Bruker AMX 300 or Bruker AMX 500 at 125.77 MHz. Deuterated methanol (Methanol-d_4) was used as the solvent for H_2Pors **3** (which provided the best overall spectrum resolution among the tested solvents), with tetramethylsilane (TMS) as the internal reference. Chemical shifts are reported in δ (ppm) and coupling constants (J) in Hertz (Hz).

Electrospray ionization-mass spectrometry (ESI-MS) spectrum was obtained using a Q-TOF 2 instrument (Micromass, Manchester, UK). Sample solutions at a concentration of 1 mg/mL were prepared by dissolving each compound in CH_2Cl_2/MeOH (95:5) or MeOH. A 2 μL aliquot of these solutions was then diluted with 200 μL of methanol containing 0.1% formic acid for direct ESI analysis, utilizing nitrogen as the nebulizer gas. The final samples were inserted into the mass spectrometer at a flow rate of 10 μL/min. The needle voltage was maintained at 3000 V, with the ion source temperature set to 80 °C and the desolvation temperature at 150 °C. Spectra were recorded at a cone voltage of 30 V, and data acquisition was performed using the Micromass MassLynx 4 software. HRMS was recorded on an APEXQe FT-ICR mass spectrometer (Bruker Daltonics, Billerica, MA).

The absorption spectra were recorded using a Shimadzu UV-2501-PC spectrophotometer with dimethylformamide (DMF) as the solvent. Steady-state fluorescence spectra were obtained on a computer-controlled Horiba Jobin Yvon FluoroMax-3 spectrofluorometer in DMF, using 1 × 1 cm quartz optical cells under normal atmospheric conditions. The fluorescence quantum yields (Φ_F) were measured between 600 and 800 nm following excitation at 418 nm, with an optical density (OD) of ~0.3. The values were calculated by comparing the integrated emission areas of these derivatives with that of 5,10,15,20-tetraphenylporphyrin (**H_2TPP**, $\Phi_F = 0.11$ in DMF) as the standard [43].

2.2. Synthesis and characterization of photosensitizer

2.2.1. 5,10,15,20-Tetrakis(4-dicarboxyethylthio-2,3,5,6-tetrafluorophenyl)porphyrin, H_2Por 3

In a 25 mL round-bottom flask, 5,10,15,20-tetrakis(pentafluorophenyl)porphyrin (**H_2TPPF$_{20}$**, 300.1 mg, 0.308 mmol, 1 equiv.), mercaptosuccinic acid (188.8 mg, 1.257 mmol, 4.1 equiv.), and K_2CO_3 (174.2 mg, 1.260 mmol, 4.1 equiv.) were mixed in 3 mL of DMF. The reaction was stirred for 24 h at room temperature. Afterward, the reaction mixture was neutralized with some drops of citric acid and the product was dropwise precipitated using pure chloroform. The solid was filtrated and recrystallized in a mixture of MeOH/$CHCl_3$. The obtained

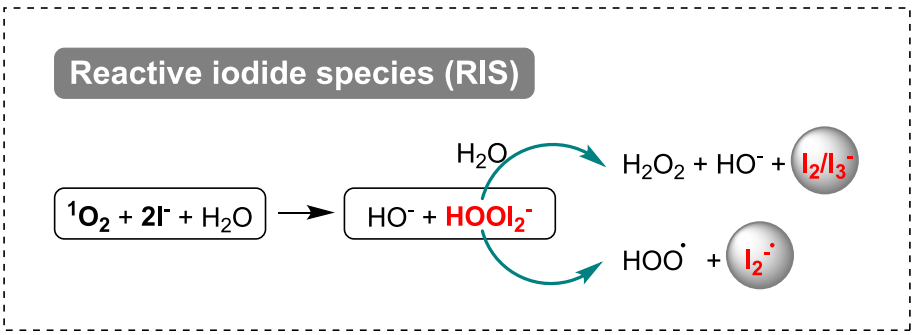

Fig. 1. Decomposition of $HOOI_2^-$, formed through the reaction between $^1O_2$ and KI.

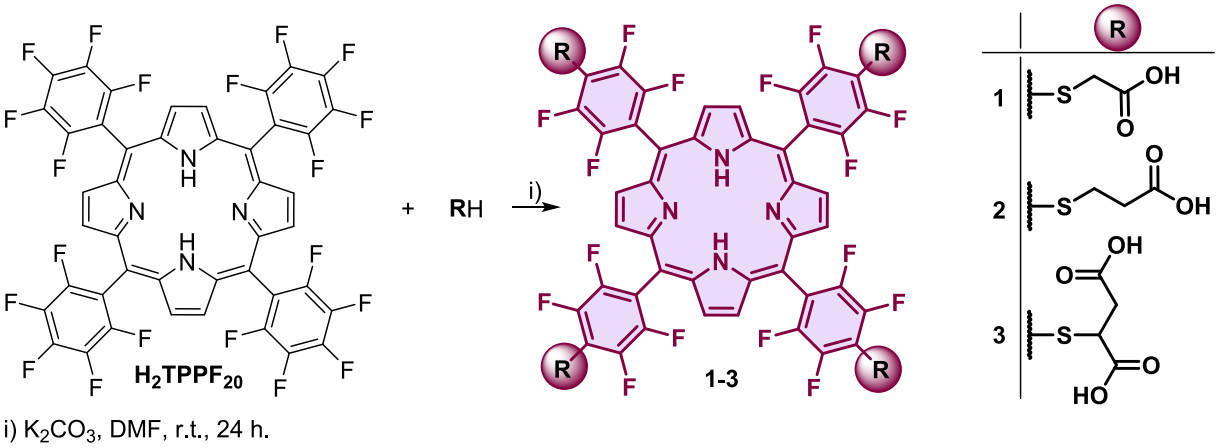

Scheme 1. Synthesis of the thiocarboxylated porphyrins H_2Pors **1**–**3**.

purple crystals were filtrated, dried in a vacuum system, and the desired compound was obtained in 57.9% (267.5 mg, 0.179 mmol) yield. ^{1}H NMR (300.13 MHz, Methanol-d_4): δ 3.08 (d, $J = 7.1$ Hz, 4H, -CH_2), 3.19 (d, $J = 7.1$ Hz, 4H, -CH_2), 4.45 (dd, $J = 8.2$, 5.8 Hz, 4H, -SCH), 7.97 (s, 8H, β-H), 9.14–9.30 (br s, 8H, -COOH) ppm. ^{19}F NMR (282. MHz, Methanol-d_4): δ − 163.22 (dd, $J = 24.7$, 11.8 Hz, 8F, Ar-*m*-F), −157.16 (dd, $J = 24.7$, 11.8 Hz, 8F, Ar-*o*-F) ppm. ^{13}C NMR (125.77 MHz, Methanol-d_4): δ 105.8, 115.6, 122.9, 129.9, 135.9, 139.1, 146.7, 148.3, 148.7, 150.3, 157.0, 170.2, 174.6, 175.1 ppm. HRMS (ESI) *m/z*: calcd for $C_{60}H_{30}F_{16}N_4O_{16}S_4$ $[M + H]^+$: 1494,02842; found 1495,03029. UV–Vis (DMF), λ_{max} (log ε): 414 (5.57), 505 (4.56), 580 (4.17) nm.

2.3. Singlet oxygen generation studies

The singlet oxygen quantum yields (Φ_Δ) were determined to evaluate the ability to generate $^1O_2$ species by monitoring the photooxidation of 9,10-dimethylanthracene (9,10–DMA), a $^1O_2$ quencher [44,45]. Solutions in DMF ($Abs_{420} \sim 0.3$) were irradiated in quartz cuvettes with monochromatic light ($\lambda = 420$ nm) in the presence of 9,10–DMA (30 μM). **H_2TPP** was used as a reference ($\Phi_\Delta = 0.65$ in DMF) [46]. The kinetics of 9,10–DMA photooxidation was studied by following the decrease in its absorbance at 378 nm, and the result registered in a first-order plot for the photooxidation of 9,10–DMA photosensitised by each tested compound, and **H_2TPP** in DMF. The kinetics of 9,10–DMA photooxidation in the absence of any compound was also studied in DMF. The results are expressed as mean and standard deviation from three independent experiments.

Furthermore, the Φ_Δ was determined by the equation indicated below:

$$\Phi_\Delta = \Phi_\Delta^{ref} \frac{K_{sample}}{K_{ref}} \frac{1 - 10^{-Abs_{ref}}}{1 - 10^{-Abs_{sample}}}$$

where Φ_Δ^{ref} is the singlet oxygen quantum yield of **H_2TPP**, K_{sample} and K_{ref} are the photodecay constant of 9,10–DMA in the presence of the sample and the reference, respectively; Abs_{sample} and Abs_{ref} are the absorbance of the sample and the reference at 420 nm.

2.4. Stability and photostability studies

Phosphate-buffered saline (PBS) solutions of each PS were freshly prepared in quartz cuvettes and the corresponding absorbances at the Soret band were adjusted between OD of ~0.2 ($\lambda_{exc.} = 418$ nm). Then, the PS solutions were irradiated under white light at an irradiance of 50 mW.cm^{-2}, and the absorbance at the correspondent S band was registered before (time $t_0 = Abs_0$) and after light irradiation (Abs_t) up to 60 min (light dose of 180 J.cm^{-2}):

$$Photostability\ (\%) = \left(\frac{Abs_t}{Abs_0}\right) \times 100$$

The white light irradiation at an irradiance of 50 mW.cm^{-2} was delivered by a white light (400–700 nm), emitted by a LED system (LUMECO, 30 W, 2000 lm).

Similar experiments were done to verify the stability of the PS solutions without light irradiation. In this case, the cuvettes were kept dark during all the experimental periods.

2.5. Solubility studies

The solubility of each PS in PBS was assessed by UV–Vis spectroscopy. Concentrations, between 0.5 and 20.0 μM, obtained by the addition of aliquots of each PS stock solution (500 μM), were analyzed. The intensity of the S band *versus* PS concentration was plotted in a graphic for linear regression to determine if these concentrations follow the Beer-Lambert law.

2.6. Biological studies

2.6.1. Bacterial strains and growth conditions

For the biological assays, the bacterial strains *S. aureus* (DSM 25693 (DSMZ-German Collection of Microorganisms and Cell Cultures GmbH, Braunschweig, Germany) and a genetically transformed bioluminescent *E. coli* [47] were selected as Gram-positive and Gram-negative bacterial models, respectively. The use of bioluminescent *E. coli* allows the monitoring of the PDI efficacy of the selected PS in real time. The correlation between CFU mL^{-1} and the bioluminescence signal emitted by *E. coli* has been established and reported in previous studies [48,49]. In those works, a strong linear relationship was demonstrated over several orders of magnitude, with reductions in relative light units (RLU) consistently mirroring the decrease in viable cell counts determined by plate enumeration (with a concentration of ≈ 10^8 CFU mL^{-1} corresponding to ~10^8 RLU). These findings validated the use of bioluminescence as a reliable and quantitative proxy for bacterial viability under comparable photodynamic inactivation conditions.

S. aureus was maintained in the laboratory on tryptic soy agar (TSA, Liofilchem, Roseto degli Abruzzi, Italy) at 4 °C. Before each test, one colony was transferred to 30 mL of tryptic soy broth medium (TSB, Liofilchem, Roseto degli Abruzzi, Italy) and then incubated at 37 °C for 18 h with stirring (120 rpm). Then, 300 μL of the previously grown bacterial suspension was transferred to 30 mL of fresh TSB medium and incubated under the above conditions to promote bacterial growth to the stationary phase (approximately 10^9 colonies forming units per millilitre (CFU.mL^{-1}).

Suspensions of *E. coli* were stored at −80 °C in 10% glycerol. Before

each test, a suspension of *E. coli* was aseptically inoculated into 30 mL of TSB and grown for 18 h at 25 °C with orbital shaking at 120 rpm. An aliquot (300 μL) of each bacterial culture was then transferred to 30 mL of fresh TSB and grown for 18 h at 25 °C with orbital shaking (120 rpm) until a stationary phase of 10^9 relative light units (RLU) was reached.

2.6.2. Photosensitizer and KI stock solutions

The thiocarboxylated PSs **1**–**3** or combined PSs **1**–**3**+KI were examined on PDI of *S. aureus* and *E. coli* bacteria. Dimethyl sulfoxide (DMSO) stock solutions of the PSs were prepared at a concentration of 500 μM, stored in the dark, and kept refrigerated at 4 °C until further use. Before each assay, the PS stock solutions were brought to room temperature and subjected to 30 min of sonication to ensure the solution's uniformity. KI (Sigma–Aldrich) solutions were prepared at 5 M in sterile distilled water immediately before each PDI assay.

2.6.3. Irradiation conditions

To conduct the PDI assays, a white light source with a specific irradiance output was utilized to investigate the impact of this parameter on the inactivation rate of the PSs being tested. The light source employed was a white LED system (Lumeco Light, 30 W, 2000 lm) that emitted light in the range of 400 to 700 nm. The irradiance was maintained at a constant value of 50 mW cm^{-2} throughout the experiments. To ensure accuracy, the irradiance was adjusted during the preparation of each assay using a power meter FieldMaxII-Top in combination with a Coherent PowerSens PS19Q energy sensor (Coherent, Santa Clara, CA, USA).

2.6.4. Antimicrobial photoinactivation experiments

To evaluate the PDI efficiency of H_2Pors **1**–**3** against *S. aureus* and *E. coli*, these PSs were tested at concentrations of 1.0 and 10.0 μM, respectively. The H_2Pors **1**–**3** efficacy was also tested in combination with KI at 100 mM. Antimicrobial photoinactivation experiments were performed under white light irradiation (400–700 nm) for 30 min at an irradiance of 50 mW cm^{-2} (total light dose of 90 J.cm^{-2}), and at a controlled temperature of 18 °C.

2.6.4.1. Antimicrobial photoinactivation of S. aureus. The bacterial culture (approximately 10^9 CFU.mL^{-1}) of *S. aureus* was diluted in PBS to a final concentration of 10^7 CFU mL^{-1}. The bacterial suspension was evenly distributed in 24–well plates, and an appropriate volume of each PS was added to achieve final concentration of 1.0 μM. Simultaneously to the treated samples, light and dark controls (LC and DC, respectively) were also included in the experiments: LC and KI light control (LC+KI) contained the bacterial suspension alone or with KI, respectively, and were submitted to the same irradiation protocol used for the samples; DC containing the bacterial cells suspension incubated with the PS combined with KI were protected from light with aluminum foil during the experiments. Samples and controls were left in the dark under stirring for 15 min at room temperature to promote PS binding to bacterial cells. Samples and LCs were then exposed to white light at 50 mW cm^{-2} for 30 min at room temperature. Dark controls were incubated without light for 30 min at room temperature. Aliquots of samples and controls were collected at time zero after 5, 10, 15, and 30 min of irradiation. Bacterial concentration was determined in triplicate in a solid TSA medium using the drop plate method after 24 h of incubation at 37 °C. Results were expressed as CFU mL^{-1}. Three independent assays with three replicates were performed for each condition. The detection limit of the colony count method was 2 log CFU/mL.

2.6.4.2. Antimicrobial photoinactivation of E. coli. An overnight *E. coli* culture (approximately 10^9 RLU) was diluted in PBS to a final bioluminescence of 10^7 RLU (corresponding to a concentration of 10^7 CFU mL^{-1}). The bacterial suspension was evenly distributed in 6-well plates. Appropriate PS or PS+KI volumes were added to the bacterial suspensions to achieve a final concentration of PS at 10.0 μM and KI at 100 mM. Simultaneously, light and dark controls were performed as previously described. Samples and controls were incubated in the dark for 15 min, stirring at room temperature to promote PS binding to *E. coli* cells. Subsequently, samples and LCs were irradiated for 30 min, stirring at room temperature, while dark controls were shielded from light. Aliquots of samples and controls were collected at intermediate times of light exposure, and the bioluminescence signal of bacteria was measured in a luminometer (TD220/20 Luminometer, Turner Designs, Inc., USA). Three independent experiments with three replicates were carried out. All the PDI assays were performed in a climatised room, maintaining its temperature at 18 ± 2 °C. The detection limit of the bioluminescence method was 2.3 log RLU.

2.7. Statistical analysis

The statistical analysis was conducted using the GraphPad Prism 8.0 software. To evaluate the normal distribution of the data, the Kolmogorov-Smirnov test was employed, while the homogeneity of variances was assessed using the Brown-Forsythe test. Differences among the tested conditions and their respective controls at each time point were analyzed using two-way analysis of variance (2way-ANOVA), followed by Tukey's multiple comparisons test. Differences corresponding to $p < 0.05$ were considered significant. Three independent assays were conducted for each condition, with duplicate technical replicates in each assay. For *S. aureus*, values below the detection limit were assigned a value of 0 for statistical analysis. For *E. coli*, values below the detection limit were assigned the luminescence value corresponding to the detection limit of the instrument (2.3 log).

3. Results

There is a pressing need to develop rapid and efficient methods for (photo)inactivating microorganisms while ensuring the protection of host cells and of the environment. Therefore, identifying highly effective PS at minimal concentrations is paramount. Given the high reactivity of **H_2TPPF$_{20}$** toward nucleophiles, we highlighted here the formation of tetra-substituted thiocarboxylate derivatives. The selective displacement of the *para*-fluorine groups in **H_2TPPF$_{20}$** by thiocarboxylic acids demonstrates that **H_2TPPF$_{20}$** is an ideal platform for the rapid formation of the dyes. Thus, H_2Pors **1** and **2** bearing different thiocarboxylate units (thioglycolic or 3-mercaptopropionic acids, respectively) were previously prepared according to the literature, each possessing four carboxylic groups [40]. This study focused for the first time on the synthesis and characterization of a new free-base porphyrin derivative bearing mercaptosuccinic acids (H_2Pors **3**, Scheme 1), possessing eight carboxylic groups. Subsequently, the properties of H_2Pors **1**–**3** were compared, and their potential as PSs for the PDI approach of *S. aureus* and *E. coli* strains was assessed.

3.1. Synthesis and structural characterization of porphyrin derivatives bearing different thiocarboxylate spacers

Considering the remarkable photochemical and -physical properties of porphyrins and the excellent features of thiocarboxylic acids to act as water soluble PSs, we envisaged simple access to new thiocarboxylate porphyrins *via* post-modification of **H_2TPPF$_{20}$**. It is noteworthy that the nucleophilic substitution of the *para*-fluorine atoms of the **H_2TPPF$_{20}$** with thiocarboxylic acids is a good methodology for preparing tetra-substituted carboxylated porphyrin dyes **1**–**3** (Scheme 1).

The tetra-carboxylated H_2Pors **1** and **2** (Scheme 1) were synthesized and structurally characterized according to the literature [40]. The new octa-carboxylated H_2Por **3** (Scheme 1) was synthesized from a reaction of **H_2TPPF$_{20}$** with four equivalents of the mercaptosuccinic acid in 3 mL of dry DMF, in the presence of an excess of K_2CO_3, from room temperature to 50 °C during 24 h. After the reaction workup, a solid was

obtained by precipitation directly from the reaction mixture. The desired product was obtained pure, after crystallization using a mixture of MeOH/$CHCl_3$/Hexane, and as a purple powder with a moderate yield (57.9%). The structure of H_2Por **3** was confirmed by ^{1}H, ^{19}F, and ^{13}C NMR (Figs. S1–S3), and UV–Vis absorption and emission spectroscopies (Fig. 2 and Table 1), as well as ESI- and FAB-HRMS (Fig. S4). The NMR spectra confirmed unequivocally the assignment of the protons, fluorine, and carbons' resonances. The mass spectrum also corroborated the substitution of four fluorine atoms in the **H_2TPPF$_{20}$**, exhibiting the typical fragmentation pathway for the type of compound.

3.2. Photochemical and photophysical properties

The absorption and emission spectra of H_2Pors **1**–**3** were recorded in DMF solutions at 298 K (Fig. 2 and Table 1). The photophysical features of these derivatives are summarized in Table 1 with the maximum wavelengths of the Soret (or S band) and Q bands, and their corresponding molar extinction coefficients. In the same table are also depicted the emission wavelength and the Φ_F for the different derivatives. All the compounds exhibited very similar absorption spectra with strong Soret band at 413–415 nm, and moderate Q bands at 505–507 and 580 nm absorptions (Fig. 2A). After excitation at 420 nm, all the compounds disclosed comparable fluorescence emission bands in the red spectral region at 600–800 nm (Fig. 2B) and the Φ_F values varied between 0.13 and 0.31 (Table 1).

The Φ_F values of H_2Pors **1**–**3** (Table 1) were determined in DMF at room temperature using optically diluted samples and were obtained by comparison of the area below the corrected emission spectra using the unsubstituted **H_2TPP** (Φ_F = 0.11 in DMF) as standard reference [43]. The Φ_F values of the porphyrin derivatives increase in the order **H_2TPP** ($\Phi_F = 0.11$) < **3** ($\Phi_F = 0.13$) < **2** ($\Phi_F = 0.24$) < **1** ($\Phi_F = 0.31$). The results show that the number of thiocarboxylic acids affects the fluorescence quantum yields; for the tetra-carboxylate derivatives, higher yields are observed comparing with the **H_2TPP** reference. This means that the presence of the carboxylic acid functional groups on the *meso*-aryl groups notoriously affects the magnitude of the derived fluorescence emission quantum yields.

3.3. Singlet oxygen studies

$^1O_2$ is one of the significant ROS produced by this type of macrocycle during the PDI process, being the intermediate for cell damage and further cell death [50]. The Φ_Δ values of H_2Pors **1**–**3** (Table 1) were determined by the absorption decay of a 9,10–DMA solution in the presence of each compound **1**–**3**, and **H_2TPP** reference (Φ_Δ = 0.65 in DMF [46]). This process is an indirect method that allows a quantitative and qualitative evaluation of the ability of these derivatives to generate $^1O_2$ species (Fig. S5).

As shown in Table 1 (and Fig. S5), all dyes were efficient $^1O_2$ producers upon light irradiation, being H_2Por **2** (Φ_Δ = 0.63) better than H_2Por **1** (Φ_Δ = 0.49) and H_2Por **3** (Φ_Δ = 0.43) and comparable to the reference of **H_2TPP** in DMF (Φ_Δ = 0.65) [46]. The obtained Φ_Δ values are comparable to other free-base porphyrins with carboxylic groups [51], being this type of molecules investigated for antimicrobial activity [20].

3.4. Stability and photostability studies

Assessing the stability and photostability of the H_2Pors **1**–**3** is essential when exposed to an aqueous medium to evaluate their potential as PSs for PDI against bacteria. The stability and photostability of the H_2Pors **1**–**3** were evaluated in PBS by observing the decay in absorbance of their Soret band under two conditions during an essay of 60 min: in the absence of light (dark conditions) to determine stability, and after exposure to white light (400–700 nm) with an irradiance of 50 mW.cm^{-2} to assess photostability. The results are described in Table 2.

H_2Pors **1**–**3** showed high stability in the absence of light and considerable photostability when subjected to 60 min under light irradiation in PBS. The size of the spacer in the thiocarboxylic acid units (as thioglycolic, 3-mercaptopropionic, or mercaptosuccinic acids) and number of carboxylic units (four *vs.* eight) in the H_2Pors **1**–**3** (Scheme 1) did not significantly affect the porphyrin derivative's stability. The excellent stability (maximum absorption reduction of 3.7% for **3**) and substantial photostability percentages (maximum absorption reduction of 12.2% for **3**) suggest that these PS are well-suited for the PDI approach of *S. aureus* and *E. coli* bacteria. The potential self-sensitized photooxidation of dyes **1** and **2** under irradiation was monitored by absorption spectroscopy over time during the photodegradation assays. No significant decrease in the Soret band intensity or changes in the spectral profile were observed within experimental error, indicating the absence of detectable photobleaching or structural degradation. These results demonstrate that dyes **1** and **2** remain photostable under the light dose, power density, and irradiation time employed. It is noteworthy that all dye solutions were freshly prepared and were sonicated to solubilize prior to measurements, guarantying the absence of dispersion effects.

3.5. Solubility studies

It is essential to explore the concentration range where the Beer-Lambert law remains valid to evaluate the solubility behaviour of each porphyrin derivative. The solubility trends of H_2Pors **1**–**3** (Fig. S6) were

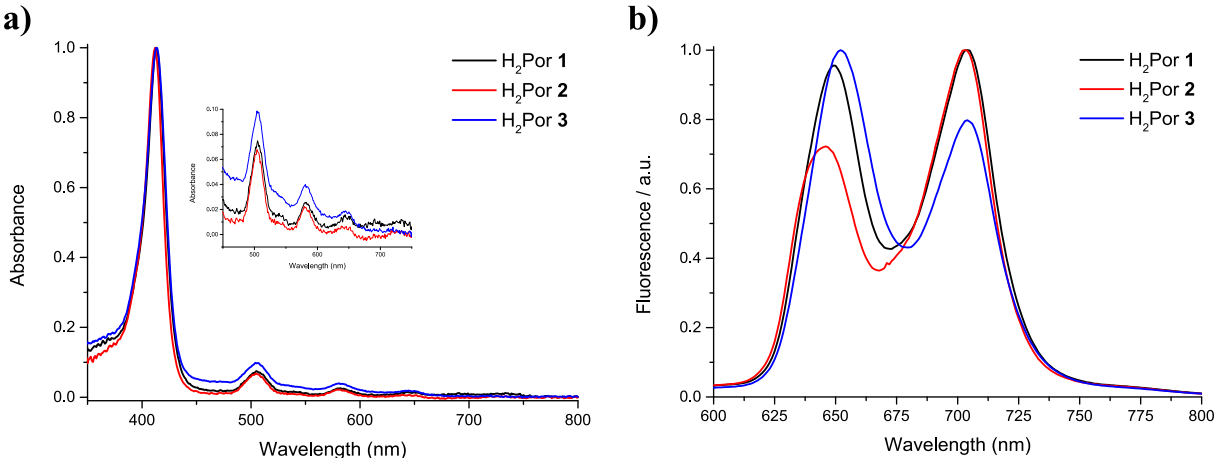

Fig. 2. Normalized spectra of a) absorption and b) emission ($\lambda_{exc.}$ = 418 nm) for H_2Pors **1**–**3** in DMF at 298 K.

Table 1
S and Q band wavelengths of maximum absorption, molar extinction coefficients (ε), fluorescence wavelengths of maximum emission ($\lambda_{emiss.}$), Φ_F and Φ_Δ of PSs **1–3** in DMF.

PS	S band λ_{max} (nm)	Q band λ_{max} (nm)	Q band λ_{max} (nm)	S band (log ε)	Q band (log ε)	Q band (log ε)	$\lambda_{emiss.}$ [a] (nm)	Φ_F [b]	Φ_Δ [c]
1	415	507	580	5.43	4.30	3.86	647/703	0.31	0.49
2	413	506	580	5.53	4.41	3.97	649/702	0.24	0.63
3	414	505	580	5.57	4.56	4.17	652/704	0.13	0.43

[a] excited at λ = 420 nm.
[b] using **H_2TPP** as reference in DMF (Φ_F = 0.11) [43].
[c] using **H_2TPP** as reference in DMF (Φ_Δ = 0.65) [46].

Table 2
Stability (dark, no light) and photostability (white light, 400–700 nm) of the H_2Pors **1–3** in PBS after 60 min under white light exposure at 50 mW.cm^{-2}.

PS	Stability (%)	Photostability (%)
1	100	100
2	100	100
3	96.3	87.8

assessed by tracking the Soret band maximum in PBS solutions over a concentration range of 0.5 to 20 μM, achieved through serial dilution from the 500 μM solution. The solubility studies revealed that H_2Pors **1–3** exhibited a high solubility behaviour within the concentration range between 0.5 and 20.0 μM.

3.6. Biological studies

The photoinactivation effect of the H_2Pors **1–3** was investigated against the *S. aureus* (Fig. 3) and *E. coli* (Fig. 4) bacteria at 1.0 and 10.0 μM, respectively, under white light irradiance of 50 mW cm^{-2} for 30 min (light doses from 0 to 90 J cm^{-2}).

Light and dark controls were performed to assess the viability of *S. aureus* and *E. coli* (Figs. 3 and 4, respectively) when exposed to white light (400–700 nm) alone (referred to as LC) or with the addition of KI (referred to as LC+KI) experiments were conducted for each assay using the tested irradiance and light dose. Additionally, dark controls with each PS+KI (referred to as DC+KI) were performed aiming to evaluate their dark toxicity. The obtained results from the light and dark controls indicated that neither white light exposure (as shown in Figs. 3 and 4) nor H_2Pors **1–3+KI** in dark have a significant effect on the *S. aureus* viability. This suggests that any antimicrobial effect observed during the PDI assays was a result of the combined action of the PS/PS+KI and their activation under white light irradiation.

All three H_2Pors **1–3** demonstrated significant activity against *S. aureus* (Anova, $p < 0.05$). Among them, H_2Por **2** exhibited the fastest kinetics, reducing bacterial counts by ~4.5 log CFU/mL within the first 5 min of treatment (Fig. 3B). H_2Por **1** also showed strong activity, with an abrupt 7.0 log reduction after 10 min (Fig. 3A), whereas H_2Por **3** was less active, but still achieved a ~ 4.5 log reduction at the same time point (Fig. 3C). Nevertheless, inactivation until the detection limit of the method was achieved for all compounds: after 10 min for H_2Pors **1** and **2** (Fig. 3A and B), and after 30 min for H_2Por **3** (Fig. 3C). The antimicrobial photoinactivation effect of all PSs was further enhanced by KI, which enabled bacterial inactivation to the detection limit of the method within just 5 min of treatment.

For *E. coli*, none of the H_2Pors **1–3** alone produced significant photoinactivation (ANOVA, $p > 0.05$) under the tested conditions (Fig. 4). However, when combined with KI, all three compounds caused inactivation to the detection limit of the method after 5, 10, and 15 min of irradiation (corresponding to total light doses of 15–45 J.cm^{-2}) with H_2Pors **1**, **3** and **2**, respectively (ANOVA, $p < 0.05$).

It is important to highlight that the previous detection limit of bioluminescent method, 2.3 log, is related with the equipment used (TD-20/20 Luminometer, Turner Designs, Inc., Madison, WI, United States), being similar to that of the colony count method, 2 log CFU/mL.

4. Discussion

In recent years, the search for more effective PDI agents has made notable progress [52]. A major factor driving this process is the incorporation of biologically inspired motifs, which enhance the therapeutic performance of PSs, particularly in the fight against microbial infections. As highlighted earlier, targeted chemical modifications of PS structures can significantly improve both selectivity and overall PDI efficiency [17]. Among the explored strategies, the conjugation of PSs with carbohydrates has emerged as a promising route for antimicrobial

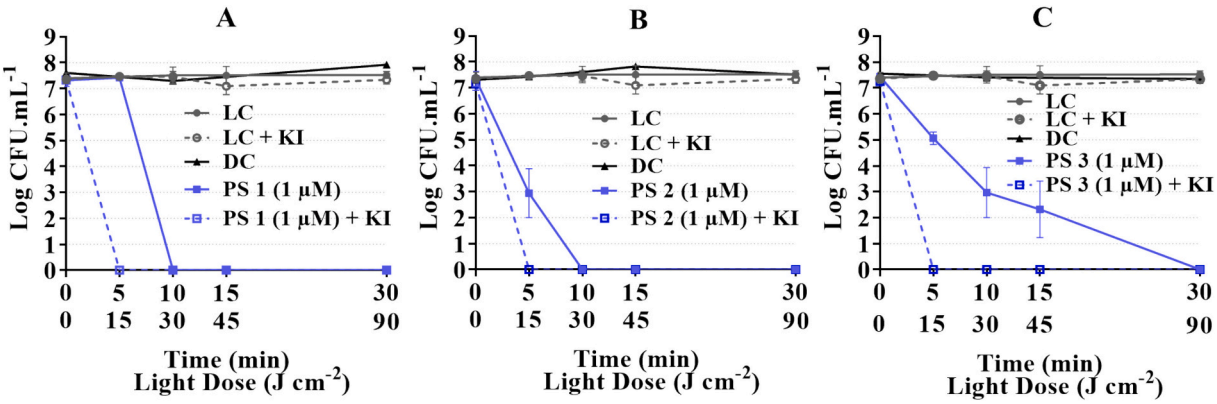

Fig. 3. PDI of *S. aureus* using each PS alone or PS+KI: A) H_2Por **1**, B) H_2Por **2**, and C) H_2Por **3** in PBS under white light exposure at 50 mW.cm^{-2}. Treatment time (min) and respective light dose (J.cm^{-2}) are presented on the X-axis. Data points represent the average of three independent experiments; error bars represent the standard deviation and in some cases are collapsed with the symbols. LC: Light control; LC+KI: Light control plus KI at 100 mM; DC: Dark Control; .PS: Sample treated with PS at 10.0 μM; PS+KI: Sample treated with PS at 10.0 μM plus KI at 100 mM.

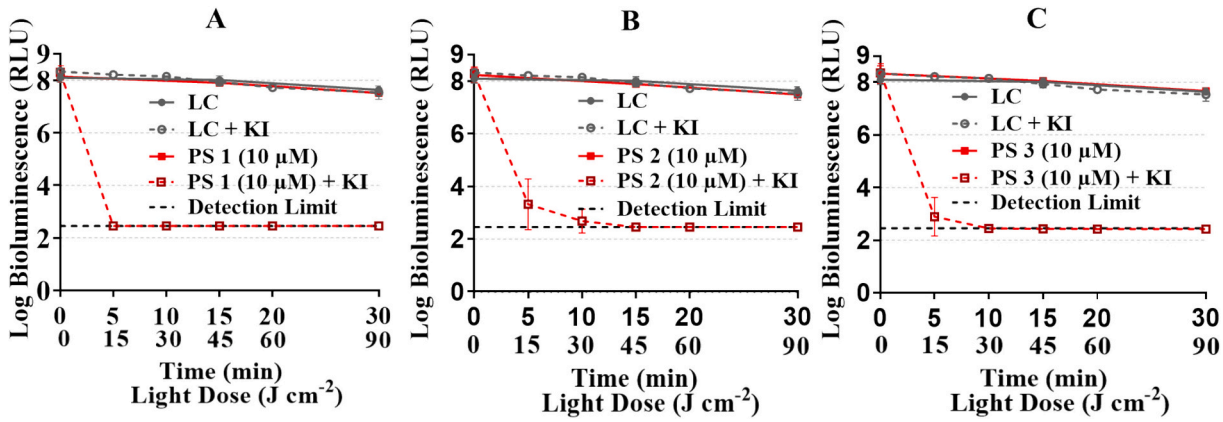

Fig. 4. PDI of *E. coli* using each PS alone or PS+KI: A) **1**, B) **2**, and C) **3** in PBS under white light exposure at 50 mW.cm^{-2}. Treatment time (min) and respective light dose (J.cm^{-2}) are presented on the X-axis. Data points represent the average of three independent experiments; error bars represent the standard deviation and in some cases are collapsed with the symbols. LC: Light control; LC+KI: Light control plus KI at 100 mM; PS: Sample treated with PS at 10.0 μM; PS+KI: Sample treated with PS at 10.0 μM plus KI at 100 mM.

inactivation [53]. Ribeiro et al. [53,54] further demonstrated that PS–cyclodextrin assemblies can enhance photodynamic activity, thereby intensifying PS-induced toxicity toward bacterial targets. In parallel, the introduction of multi-hydroxyl groups, for instance through carboxyl [20], thioglycerol [21], or galactodendritic [55] moieties, has been proposed as an effective means to fine-tune the lipophilicity of various dye systems. Additionally, several studies have also explored photodynamic antimicrobial strategies, food preservation, antimicrobial coatings, and light-activated microbial control [23–29].

The introduction of multiple carboxylic acid groups in these porphyrin derivatives is expected to enhance water solubility for biomedical and environmental applications. For this reason, we performed solubility/aggregation studies for all three photosensitizers in PBS (Fig. S6) under the same experimental conditions used in the PDI assays. These results are in accordance with the Beer-Lambert's law. As shown there, the Soret band intensity ($\lambda = 410$ nm) varies linearly with concentration for H_2Pors **1**–**3** (from 0.5 to 20.0 μM), indicating that no significant aggregation occurs in PBS within the concentration range employed in the biological experiments. To assess their antimicrobial performance, we conducted *in vitro* PDI experiments against both Gram-positive (*S. aureus*) and Gram-negative (*E. coli*) bacteria using H_2Pors **1**–**3** (1–10 μM), either alone or in combination with KI salt (100 mM). Antimicrobial efficacy was quantified by monitoring the reduction in bacterial viability (log scale) after exposure to white light for 30 min (50 mW cm^{-2}; light doses from 0 to 90 J cm^{-2}). It is noteworthy that neither light exposure alone nor the presence of the PS at its highest concentration compromised bacterial viability, and no dark cytotoxicity was observed. Additionally, it is important to note that the KI addition is well-documented to potentiate the PDI activity of diverse PSs, and the concentration employed here was selected in accordance with previous studies [35].

All three H_2Pors **1**–**3** displayed significant photodynamic activity against *S. aureus* (ANOVA, $p < 0.05$). H_2Por **2** showed the fastest response, achieving a ~4.5 log CFU/mL reduction within 5 min of treatment (light dose of 15 J.cm^{-2}, Fig. 3B). H_2Por **1** also proved highly effective, producing a sharp 7.0 log decrease after 10 min (light dose of 30 J cm^{-2}, Fig. 3A). In contrast, H_2Por **3** was comparatively less potent, though it still achieved a ~4.5 log reduction at the 10 min mark (light dose of 30 J.cm^{-2}, Fig. 3C). Despite these differences in kinetics, inactivation to the detection limit of the method was ultimately observed for all compounds: after 10 min for H_2Pors **1** and **2** (light dose of 30 J.cm^{-2}) and after 30 min for H_2Por **3** (light dose of 90 J cm^{-2}). Notably, H_2Por **2** acted most rapidly, followed by H_2Por **1** and H_2Por **3**, highlighting that Φ_Δ alone does not fully predict PDI efficacy. These findings reinforce the importance of considering molecular architecture in designing efficient photosensitizers [56].

The addition of KI substantially enhanced the photodynamic effect across all PSs, reducing both treatment time and light dose required for bactericidal activity. This enhancement is consistent with the formation of RIS (such as H_2O_2, I_2/I_3^-, and $I_2^{-\bullet}$) through $^1O_2$-mediated iodide oxidation, as previously reported [57]. All PSs was still able to inactivate *S. aureus* by more than 3 Log CFU/mL at 1 μM after light treatment, meeting the requirement to be considered bactericidal. Overall, these results demonstrate that multi-carboxylated porphyrins, particularly in combination with KI, provide a versatile platform for efficient antimicrobial photodynamic applications, aligning with current strategies for improving PS performance through structural optimization and adjuvant use [58].

Against *E. coli*, none of the H_2Pors **1**–**3** alone induced significant photoinactivation under the tested conditions (Fig. 4). In contrast, the addition of KI transformed their activity, enabling all three compounds to achieve inactivation to the detection limit of the method (ANOVA, $p < 0.05$) after 5 min with H_2Por **1**, 10 min with H_2Por **3**, and 15 min with H_2Por **2**, corresponding to light doses of 15, 30, and 45 J cm^{-2}, respectively. In line with previous reports, none of the tested derivatives alone produced significant photoinactivation of *E. coli* at 10 μM after 30 min of irradiation. This behaviour is attributed to the limited interaction between neutral PSs and the negatively charged outer membrane of Gram-negative bacteria. Because $^1O_2$ has both a short lifetime and a restricted diffusion range, ineffective binding of the PSs prevents efficient bacterial inactivation. By contrast, Gram-positive bacteria are more susceptible: their thick but porous peptidoglycan layer allows neutral PSs to penetrate and exert their PDI effect [59]. The resilience of *E. coli* was effectively overcome by the addition of KI, which boosted the activity of all derivatives and drove photoinactivation down to the detection limit of the assay within just 5–15 min of light exposure (Fig. 4).

Although $^1O_2$ production is one of the important factors to consider in the photoinactivation of pathogenic microorganisms, in this case, the obtained values for Φ_Δ are relatively high (H_2Por **3**, $\Phi_\Delta = 0.43$ < H_2Por **1**, $\Phi_\Delta = 0.49$ < H_2Por **2**, $\Phi_\Delta = 0.63$ < **H_2TPPF$_{20}$**, $\Phi_\Delta = 0.65$). As previously described, all porphyrins produce $^1O_2$ species, with H_2Por **2** presenting a comparable Φ_Δ value relatively to the reference of **H_2TPPF$_{20}$**, following H_2Por **1** and H_2Por **3**, respectively. The $^1O_2$ production values of the PS alone align with the PDI profile observed in *S. aureus*, but this correlation is not observed in *E. coli*, indicating that Φ_Δ is not the sole determinant of PDI efficacy in the combined systems of PS+KI. Although the three porphyrins display similar photophysical properties, including comparable Φ_Δ values, our results indicate that Φ_Δ alone does not determine PDI efficiency. The superior antibacterial

performance of H_2Por **2** is most likely related to structural factors that influence its interaction with bacterial surfaces. Specifically, the longer and more flexible -CH_2CH_2COOH substituent in H_2Por **2** provides a more favourable balance to enhance molecular accessibility and binding to the bacterial envelope compared with the shorter –CH_2COOH chain in H_2Por **1**. In contrast, H_2Por **3** carries eight carboxylate groups and is considerably bulkier, which likely introduces steric hindrance and reduces its ability to approach and interact efficiently with bacterial targets. These combined structural effects support our conclusion that PDI efficacy arises from the interplay between photophysical behaviour and the molecular architecture governing PS–bacteria interactions, rather than from Φ_Δ alone. Additionally, it will be important in future studies to analyse the binding affinity and cellular uptake for H_2Pors **1**–**3**. However, our results are consistent with earlier reports showing that additional structural properties of photosensitizers play a decisive role in shaping the effectiveness of the PS+KI synergistic PDI strategy. For example, Tomé et al. demonstrated that diketopyrrolopyrroles with low Φ_Δ values ($\leq$4%) – ineffective against *E. coli* on their own – became highly potent when used in combination with KI [60]. Likewise, another work revealed that two porphyrinic isomers with similar Φ_Δ values displayed strikingly different activities. This contrast was attributed to variations in charge distribution, which influenced bacterial binding and, consequently, the extent of RIS-mediated damage [61]. Indeed, the PS+KI synergistic effect likely arises from a multifactorial interplay involving the PS's structural features, its charge characteristics, and its affinity toward microbial cells. Incorporating carboxylic groups into porphyrin derivatives may improve water solubility and boost antimicrobial efficacy, our tested tetrapyrrolic derivatives of H_2Pors **1**–**3**+**KI** evidenced great performance. Thus, it was observed an effective viability reduction of the bacteria given that they present high level of Φ_Δ, stability/photostability, and solubility.

The potentiation of the antimicrobial photoinactivation by KI is generally attributed to the oxidation of I^- by $^1O_2$ and/or other ROS generated under light irradiation. This process leads to the formation of RIS. It is noteworthy that the RIS mechanism is a plausible explanation supported by previous studies rather than a mechanism directly demonstrated here. These species are longer-lived and more diffusible than $^1O_2$, which allows them to extend the antimicrobial effect beyond the immediate vicinity of the PS. Additionally, RIS may penetrate microbial cells more efficiently and contribute to oxidative damage of proteins, lipids, and nucleic acids, thereby amplifying the overall photodynamic effect. Although the enhanced antimicrobial efficacy observed in the presence of KI (100 mM) highlights the potential of this approach, the present findings should be interpreted within the limitations of the experimental design, which was restricted to planktonic bacterial suspensions in PBS. Therefore, further studies are required before clinical translation, or environmental applications can be considered. In our recent work [62], KI concentrations above 10 mM induced toxicity in the aquatic models *Artemia franciscana* and *Scophthalmus maximus* L., indicating that the environmental impact of KI should be carefully considered in applications that may result in its release into aquatic ecosystems. Nevertheless, previous *in vivo* studies [63,64] have demonstrated that KI concentrations of 100 mM or higher, when combined with photosensitizers, were well tolerated in murine models and successfully treated candidiasis and urinary tract infections without detectable adverse effects. These findings support the continued investigation of KI-potentiated antimicrobial photodynamic therapy for clinical applications. Future studies should focus on evaluating cytotoxicity toward mammalian cells, *in vivo* tolerance, dose optimization, and the performance of this strategy in more complex biological matrices.

While the results obtained with the combination of PS+KI in planktonic *S. aureus* and *E. coli* are promising, the antimicrobial performance of H_2Pors **1**–**3** against multidrug-resistant pathogens, biofilms, and other clinically relevant microbial models remains to be investigated. Therefore, the potential applicability of these photosensitizers in more complex biological settings should be considered preliminary until supported by further experimental evidence.

5. Conclusions

The H_2Por **3** was obtained *via* selective replacement of the *para*-fluorine atoms of the **H_2TPPF$_{20}$** with mercaptosuccinic acid units; and compared with the previous reported H_2Pors **1** and **2**. All dyes are stable and photostable under white light irradiation and have higher fluorescence quantum yields (Φ_F = 0.13–0.31), generating $^1O_2$ species (Φ_Δ = 0.43–0.63), which explain their effectiveness against *S. aureus* and *E. coli,* Gram-positive and Gram-negative bacterial models, respectively, mainly in the presence of KI. Interestingly, the photoinactivation performance in the absence and presence of KI, indicated that Φ_Δ is not the sole determinant of PDI efficacy in the single PS or combined PS+KI systems. This observation is consistent with previous reports showing that structural features of PSs, such as charge distribution, size and type of spacer (four *vs* eight carboxylic units), and bacterial affinity, play a crucial role in influencing the PDI outcome.

Considering the high efficiency of the H_2Pors **1**–**3**+**KI** on the inactivation of *S. aureus* and *E. coli* (>3 Log RLU), according to the guidelines of the American Society for Microbiology, these PSs+KI can be considered effective antibacterial agents. The potential of these PSs is magnified with the requirement of low concentrations and low light doses to achieve effective inactivation of both bacterial planktonic forms, which is a clear advantage for their application.

CRediT authorship contribution statement

Leandro M.O. Lourenço: Writing – review & editing, Validation, Supervision, Resources, Investigation, Formal analysis, Conceptualization. **Cátia Vieira:** Writing – original draft, Validation, Methodology, Investigation, Formal analysis. **Duarte Rosa:** Methodology, Investigation. **Maria Bartolomeu:** Investigation. **Adelaide Almeida:** Writing – review & editing, Validation, Supervision, Resources, Funding acquisition, Formal analysis.

Funding

This work received financial support from PT national funds (FCT/MCTES, Fundação para a Ciência e a Tecnologia and Ministério da Ciência, Tecnologia e Ensino Superior) through projects LAQV-REQUIMTE (UID/50006/2025, DOI: 10.54499/UID/50006/2025), CESAM (UID/50006 +LA/P/0094/2020, DOI: 10.54499/LA/P/0094/2020), and COMPETE2030-FEDER-00799000. C. Vieira thanks FCT for their PhD grant (SFRH/BD/150358/2019).

Declaration of competing interest

The authors declare that they have no known competing financial interests or personal relationships that could have appeared to influence the work reported in this paper.

Acknowledgements

Thanks to the University of Aveiro and FCT/MCTES (Fundação para a Ciência e a Tecnologia and Ministério da Ciência, Tecnologia e Ensino Superior) for the financial support to LAQV-REQUIMTE (UID/50006/2025, DOI: 10.54499/UID/50006/2025), CESAM (UID/50006+LA/P/0094/2020, DOI: 10.54499/LA/P/0094/2020), and COMPETE2030-FEDER-00799000 funded by FCT/MCTES through national funds. C. Vieira thanks FCT for their PhD grant (SFRH/BD/150358/2019).

Appendix A. Supplementary data

Supplementary data to this article can be found online at https://doi.

org/10.1016/j.jphotochem.2026.117661.

Data availability

Data will be made available on request.

References

[1] S.K. Ahmed, S. Hussein, K. Qurbani, R.H. Ibrahim, A. Fareeq, K.A. Mahmood, M. G. Mohamed, Antimicrobial resistance: impacts, challenges, and future prospects, J. Med. Surg. Public Health 2 (2024) 100081, https://doi.org/10.1016/j.glmedi.2024.100081.

[2] M.J. Bottery, J.W. Pitchford, V.-P. Friman, Ecology and evolution of antimicrobial resistance in bacterial communities, ISME J. 15 (2021) 939–948, https://doi.org/10.1038/s41396-020-00832-7.

[3] M.R. Hamblin, H. Abrahamse, Can light-based approaches overcome antimicrobial resistance? Drug Dev. Res. 80 (2019) 48–67, https://doi.org/10.1002/ddr.21453.

[4] S.R.D. Gamelas, C. Vieira, M. Bartolomeu, M.A.F. Faustino, J.P.C. Tomé, A. C. Tomé, A. Almeida, L.M.O. Lourenço, Photodynamic inactivation of pathogenic gram-negative and gram-positive bacteria mediated by Si(IV) phthalocyanines bearing axial ammonium units, J. Photochem. Photobiol. B 233 (2022) 112502, https://doi.org/10.1016/j.jphotobiol.2022.112502.

[5] S.R.D. Gamelas, M. Bartolomeu, T.J. Gomes, M.A.F. Faustino, J.P.C. Tomé, A. C. Tomé, A. Almeida, A.T.P.C. Gomes, L.M.O. Lourenço, Photodynamic inactivation of a RNA-virus model using water-soluble β-octa-substituted pyridinium-pyrazolyl phthalocyanines, Dyes Pigments 220 (2023) 111661, https://doi.org/10.1016/j.dyepig.2023.111661.

[6] M.T. Islam, M. Sain, C. Stark, M. Fefer, J. Liu, T. Hoare, W. Ckurshumova, C. Rosa, Overview of methods and considerations for the photodynamic inactivation of microorganisms for agricultural applications, Photochem. Photobiol. Sci. 22 (2023) 2675–2686, https://doi.org/10.1007/s43630-023-00466-6.

[7] A.K. Surur, A.B. de Oliveira, S.R. De Annunzio, T.M. Ferrisse, C.R. Fontana, Bacterial resistance to antimicrobial photodynamic therapy: a critical update, J. Photochem. Photobiol. B 255 (2024) 112905, https://doi.org/10.1016/j.jphotobiol.2024.112905.

[8] I. Santos, S.R.D. Gamelas, C. Vieira, M.A.F. Faustino, J.P.C. Tomé, A. Almeida, A.T. P.C. Gomes, L.M.O. Lourenço, Pyrazole-pyridinium porphyrins and chlorins as powerful photosensitizers for photoinactivation of planktonic and biofilm forms of *E. coli*, Dyes Pigments 193 (2021) 109557, https://doi.org/10.1016/j.dyepig.2021.109557.

[9] D.N. Maronde, C. Vieira, J.E. Rodríguez-Borges, A. Almeida, L.M.O. Lourenço, *Staphylococcus aureus* and *Escherichia coli* inactivation through mercaptophenylboronic acid-functionalized fluorinated porphyrin, Dyes Pigments 246 (2026) 113429, https://doi.org/10.1016/j.dyepig.2025.113429.

[10] J.M.D. Calmeiro, C.J. Dias, C.I.V. Ramos, A. Almeida, J.P.C. Tomé, M.A. F. Faustino, L.M.O. Lourenço, Comparative photodynamic inactivation of bioluminescent *E. Coli* by pyridinium and inverted pyridinium chlorins, Dyes Pigments 173 (2020) 107410, https://doi.org/10.1016/j.dyepig.2019.03.021.

[11] S.R.D. Gamelas, C. Pereira, M.A.F. Faustino, A. Almeida, L.M.O. Lourenço, Unveiling the potent antimicrobial photodynamic therapy in gram-positive and gram-negative bacteria – water remediation with monocharged chlorins, Chemosphere 367 (2024) 143593, https://doi.org/10.1016/j.chemosphere.2024.143593.

[12] S.R.D. Gamelas, M. Bartolomeu, C. Vieira, M.A.F. Faustino, J.P.C. Tomé, A. C. Tomé, A. Almeida, L.M.O. Lourenço, Bacterial photodynamic inactivation: eradication of *Staphylococcus aureus* and *Escherichia coli* mediated by pyridinium-pyrazolyl zinc(II) Phthalocyanines, ACS Appl. Bio Mater. 7 (2024) 7748–7757, https://doi.org/10.1021/acsabm.4c01368.

[13] D.N. Maronde, J.E. Rodríguez-Borges, A. Almeida, L.M.O. Lourenço, Harnessing light for antimicrobial action: light-driven inactivation of gram-positive bacteria by boronic acid-based zinc(II) phthalocyanines, J. Photochem. Photobiol. A Chem. 474 (2026) 117007, https://doi.org/10.1016/j.jphotochem.2025.117007.

[14] M.R. Hamblin, T. Hasan, Photodynamic therapy: a new antimicrobial approach to infectious disease? Photochem. Photobiol. Sci. 3 (2004) 436–450, https://doi.org/10.1039/b311900a.

[15] T. Maisch, Anti-microbial photodynamic therapy: useful in the future? Lasers Med. Sci. 22 (2007) 83–91, https://doi.org/10.1007/s10103-006-0409-7.

[16] T. Dai, Y.-Y. Huang, M.R. Hamblin, Photodynamic therapy for localized infections—state of the art, Photodiagn. Photodyn. Ther. 6 (2009) 170–188, https://doi.org/10.1016/j.pdpdt.2009.10.008.

[17] S. Gnanasekar, G. Kasi, X. He, K. Zhang, L. Xu, E.-T. Kang, Recent advances in engineered polymeric materials for efficient photodynamic inactivation of bacterial pathogens, Bioact. Mater. 21 (2023) 157–174, https://doi.org/10.1016/j.bioactmat.2022.08.011.

[18] P.-C. Lo, M.S. Rodríguez-Morgade, R.K. Pandey, D.K.P. Ng, T. Torres, F. Dumoulin, The unique features and promises of phthalocyanines as advanced photosensitisers for photodynamic therapy of cancer, Chem. Soc. Rev. 49 (2020) 1041–1056, https://doi.org/10.1039/C9CS00129H.

[19] V. Almeida-Marrero, E. van de Winckel, E. Anaya-Plaza, T. Torres, A. de la Escosura, Porphyrinoid biohybrid materials as an emerging toolbox for biomedical light management, Chem. Soc. Rev. 47 (2018) 7369–7400, https://doi.org/10.1039/C7CS00554G.

[20] M. Sautour, T. Théry, G. Divoux, S. Dupont, L. Beney, C.P. Gros, N. Desbois, Synthesis and characterization of new acid-functionalized porphyrins displaying antimicrobial activity against gram positive bacteria, yeasts and filamentous fungi with or without ultra-high irradiance, Bioorg. Med. Chem. 109 (2024) 117810, https://doi.org/10.1016/j.bmc.2024.117810.

[21] L.M.O. Lourenço, S. Beirão, A. Melo, R. Fernandes, J.P.C. Tomé, Thioglycerol-porphyrin, -chlorin, and -phthalocyanine derivatives for photodynamic therapy of UM-UC-3 bladder cancer cells, J. Photochem. Photobiol. A Chem. 442 (2023) 114768, https://doi.org/10.1016/j.jphotochem.2023.114768.

[22] S.F. Musolino, F. Shatila, G.M.O. Tieman, A.C. Masarsky, M.C. Thibodeau, J. E. Wulff, H.L. Buckley, Light-induced anti-bacterial effect against *Staphylococcus aureus* of porphyrin covalently bonded to a polyethylene terephthalate surface, ACS Omega 7 (2022) 29517–29525, https://doi.org/10.1021/acsomega.2c04294.

[23] D. Pang, G. Zhou, W. Chu, X. Huang, K. Xing, B. Xu, Y. Ni, Fabrication of the high-performance label for freshness maintenance in meat products via a "three-dimensional adsorption" strategy, Food Res. Int. 238 (2026) 119411, https://doi.org/10.1016/j.foodres.2026.119411.

[24] Y. Ni, D. Pang, H. Li, G. Zhou, Y. Li, Y. Yao, B. Xu, Recent progress in typical foodborne spore-forming bacteria detection, Food Chem. 504 (2026) 147858, https://doi.org/10.1016/j.foodchem.2026.147858.

[25] H. Li, Y. Ni, Y. Li, B. Xu, Curcumin/octyl gallate/chitosan photodynamic coating with enhanced adhesion and antibacterial efficacy for preservation of prepared mutton, Innovative Food Sci. Emerg. Technol. 111 (2026) 104530, https://doi.org/10.1016/j.ifset.2026.104530.

[26] D. Pang, Y. Ni, H. Li, G. Zhou, Y. Li, B. Xu, Antimicrobial mechanism of typical microbial preservatives and its potentiation strategy by photodynamic inactivation: a review, Food Microbiol. 132 (2025) 104833, https://doi.org/10.1016/j.fm.2025.104833.

[27] Y. Li, Y. Ni, W. He, H. Li, W. Zhang, L. Tan, J. Zhao, B. Xu, Mussel-inspired highly adhesive carrageenan-based coatings with self-activating enhanced activity for meat preservation, Carbohydr. Polym. 348 (2025) 122840, https://doi.org/10.1016/j.carbpol.2024.122840.

[28] H. Li, Y. Ni, J. Zhao, Y. Li, B. Xu, Photodynamic inactivation of edible photosensitizers for fresh food preservation: comprehensive mechanism of action and enhancement strategies, Compr. Rev. Food Sci. Food Saf. 23 (2024), https://doi.org/10.1111/1541-4337.70006.

[29] Y. Ni, J. Zhao, W. Zhang, L. Tan, Y. Li, H. Li, B. Xu, Efficient fresh lamp light-harvesting films with the self-activating continuous and recyclable bactericidal ability for ultrapersistent freshness of perishable muscle food, J. Agric. Food Chem. 72 (2024) 2756–2764, https://doi.org/10.1021/acs.jafc.3c07299.

[30] T.G. St Denis, D. Vecchio, A. Zadlo, A. Rineh, M. Sadasivam, P. Avci, L. Huang, A. Kozinska, R. Chandran, T. Sarna, M.R. Hamblin, Thiocyanate potentiates antimicrobial photodynamic therapy: in situ generation of the sulfur trioxide radical anion by singlet oxygen, Free Radic. Biol. Med. 65 (2013) 800–810, https://doi.org/10.1016/j.freeradbiomed.2013.08.162.

[31] L. Huang, A. El-Hussein, W. Xuan, M.R. Hamblin, Potentiation by potassium iodide reveals that the anionic porphyrin TPPS4 is a surprisingly effective photosensitizer for antimicrobial photodynamic inactivation, J. Photochem. Photobiol. B 178 (2018) 277–286, https://doi.org/10.1016/j.jphotobiol.2017.10.036.

[32] X. Wu, Y.Y. Huang, Y. Kushida, B. Bhayana, M.R. Hamblin, Broad-spectrum antimicrobial photocatalysis mediated by titanium dioxide and UVA is potentiated by addition of bromide ion via formation of hypobromite, Free Radical Bio. Med. 95 (2016) 74–81, https://doi.org/10.1016/j.freeradbiomed.2016.03.012.

[33] C. Vieira, M. Bartolomeu, C.J.P. Monteiro, J.L. Romalde, P.P. Gallego, M.G.P.M. S. Neves, M.A.F. Faustino, A. Almeida, Cationic photosensitizers and potassium iodide: an innovative approach for enhanced photodynamic inactivation of pathogenic bacteria in aquaculture, Aquaculture 596 (2025) 741882, https://doi.org/10.1016/j.aquaculture.2024.741882.

[34] M.R. Hamblin, Potentiation of antimicrobial photodynamic inactivation by inorganic salts, Expert Rev. Anti-Infect. Ther. 15 (2017) 1059–1069, https://doi.org/10.1080/14787210.2017.1397512.

[35] C. Vieira, A. Santos, M.Q. Mesquita, A.T.P.C. Gomes, M.G.P.M.S. Neves, M.A. F. Faustino, A. Almeida, Advances in aPDT based on the combination of a porphyrinic formulation with potassium iodide: effectiveness on bacteria and fungi planktonic/biofilm forms and viruses, J. Porphyrins Phthalocyanines 23 (2019) 534–545, https://doi.org/10.1142/S1088424619500408.

[36] L. Huang, B. Bhayana, W. Xuan, R.P. Sanchez, B.J. McCulloch, S. Lalwani, M. R. Hamblin, Comparison of two functionalized fullerenes for antimicrobial photodynamic inactivation: potentiation by potassium iodide and photochemical mechanisms, J. Photochem. Photobiol. B 186 (2018) 197–206, https://doi.org/10.1016/j.jphotobiol.2018.07.027.

[37] N. Mariño-Ocampo, L. Dibona-Villanueva, E. Escobar-Álvarez, D. Guerra-Díaz, D. Zúñiga-Núñez, D. Fuentealba, J. Robinson-Duggon, Recent photosensitizer developments, delivery strategies and combination-based approaches for photodynamic therapy†, Photochem. Photobiol. 99 (2023) 469–497, https://doi.org/10.1111/php.13749.

[38] E.L. Bastos, F.H. Quina, M.S. Baptista, Endogenous photosensitizers in human skin, Chem. Rev. 123 (2023) 9720–9785, https://doi.org/10.1021/acs.chemrev.2c00787.

[39] C.P.S. Ribeiro, L.M.O. Lourenço, Overview of cationic phthalocyanines for effective photoinactivation of pathogenic microorganisms, J. Photochem. Photobiol. C Photchem. Rev. 48 (2021) 100422, https://doi.org/10.1016/j.jphotochemrev.2021.100422.

[40] L.M.O. Lourenço, J. Resende, B.A. Iglesias, K. Castro, S. Nakagaki, M.J. Lima, A. F. Da Cunha, M.G.P.M.S. Neves, J.A.S. Cavaleiro, J.P.C. Tomé, Synthesis, characterization and electrochemical properties of meso-thiocarboxylate-substituted porphyrin derivatives, J. Porphyrins Phthalocyanines 18 (2014), https://doi.org/10.1142/S1088424614500783.

[41] A. Jiblaoui, S. Leroy-Lhez, T.-S. Ouk, K. Grenier, V. Sol, Novel polycarboxylate porphyrins: synthesis, characterization, photophysical properties and preliminary antimicrobial study against gram-positive bacteria, Bioorg. Med. Chem. Lett. 25 (2015) 355–362, https://doi.org/10.1016/j.bmcl.2014.11.033.
[42] W.L.F. Armarego, C.L.L. Chai, Purification of laboratory chemicals, Seventh, Elsevier, Oxford, 2013, https://doi.org/10.1016/C2009-0-64000-9.
[43] M. Taniguchi, J.S. Lindsey, D.F. Bocian, D. Holten, Comprehensive review of photophysical parameters (ε, Φf, τs) of tetraphenylporphyrin (H2TPP) and zinc tetraphenylporphyrin (ZnTPP) – critical benchmark molecules in photochemistry and photosynthesis, J. Photochem. Photobiol. C Photchem. Rev. 46 (2021) 100401, https://doi.org/10.1016/j.jphotochemrev.2020.100401.
[44] R. Castro-Olivares, G. Günther, A.L. Zanocco, E. Lemp, Linear free energy relationship analysis of solvent effect on singlet oxygen reactions with mono and disubstituted anthracene derivatives, J. Photochem. Photobiol. A Chem. 207 (2009) 160–166, https://doi.org/10.1016/j.jphotochem.2009.05.012.
[45] A. Prostak, H.B. Mark, W.N. Hansen, Simultaneous electrochemical and internal-reflection spectrometric measurements using gold-film electrodes, J. Phys. Chem. 72 (1968) 2576–2582, https://doi.org/10.1021/j100853a054.
[46] J.C.J.M.D. S. Menezes, M.A.F. Faustino, K.T. de Oliveira, M.P. Uliana, V.F. Ferreira, S. Hackbarth, B. Röder, T. Teixeira Tasso, T. Furuyama, N. Kobayashi, A.M.S. Silva, M.G.P.M.S. Neves, J.A.S. Cavaleiro, Synthesis of new chlorin e_6 trimethyl and protoporphyrin IX dimethyl ester derivatives and their photophysical and electrochemical characterizations, Chem. Eur. J. 20 (2014) 13644–13655, https://doi.org/10.1002/chem.201403214.
[47] M.G.P.M.S. Neves, A.C. Tomé, J.A.S. Cavaleiro, Â. Cunha, S. Mendo, A. Almeida, E. Alves, C.M.B. Carvalho, J.P.C. Tomé, M.A.F. Faustino, M.G.P.M.S. Neves, A. C. Tomé, J.A.S. Cavaleiro, A. Cunha, S. Mendo, A. Almeida, Photodynamic inactivation of recombinant bioluminescent Escherichia coli by cationic porphyrins under artificial and solar irradiation, J. Ind. Microbiol. Biotechnol. 35 (2008) 1447–1454, https://doi.org/10.1007/s10295-008-0446-2.
[48] E. Alves, L. Costa, Â. Cunha, M.A.F. Faustino, M.G.P.M.S. Neves, A. Almeida, Bioluminescence and its application in the monitoring of antimicrobial photodynamic therapy, Appl. Microbiol. Biotechnol. 92 (2011) 1115–1128, https://doi.org/10.1007/s00253-011-3639-y.
[49] E. Alves, C.M.B. Carvalho, J.P.C. Tomé, M.A.F. Faustino, M.G.P.M.S. Neves, A. C. Tomé, J.A.S. Cavaleiro, Â. Cunha, S. Mendo, A. Almeida, Photodynamic inactivation of recombinant bioluminescent *Escherichia coli* by cationic porphyrins under artificial and solar irradiation, J. Ind. Microbiol. Biotechnol. 35 (2008) 1447–1454, https://doi.org/10.1007/s10295-008-0446-2.
[50] R. Boscencu, G. Manda, N. Radulea, R.P. Socoteanu, L.C. Ceafalan, I.V. Neagoe, I. F. MacHado, S.H. Basaga, L.F.V. Ferreira, Studies on the synthesis, photophysical and biological evaluation of some unsymmetrical meso-tetrasubstituted phenyl porphyrins, Molecules 22 (2017) 1–20, https://doi.org/10.3390/molecules22111815.
[51] F. Le Guern, T.-S. Ouk, I. Yerzhan, Y. Nurlykyz, P. Arnoux, C. Frochot, S. Leroy-Lhez, V. Sol, Photophysical and bactericidal properties of Pyridinium and imidazolium porphyrins for photodynamic antimicrobial chemotherapy, Molecules 26 (2021) 1122, https://doi.org/10.3390/molecules26041122.
[52] M. Grimmeisen, C. Jessen-Trefzer, Increasing the selectivity of light-active antimicrobial agents – or how to get a photosensitizer to the desired target, ChemBioChem 24 (2023), https://doi.org/10.1002/cbic.202300177.
[53] C.P.S. Ribeiro, S.R.D. Gamelas, M.A.F. Faustino, A.T.P.C. Gomes, J.P.C. Tomé, A. Almeida, L.M.O. Lourenço, Unsymmetrical cationic porphyrin-cyclodextrin bioconjugates for photoinactivation of *Escherichia coli*, Photodiagn. Photodyn. Ther. 31 (2020) 101788, https://doi.org/10.1016/j.pdpdt.2020.101788.
[54] C.P.S. Ribeiro, M.A.F. Faustino, A. Almeida, L.M.O. Lourenço, The antimicrobial photoinactivation effect on *Escherichia coli* through the action of inverted cationic porphyrin–cyclodextrin conjugates, Microorganisms 10 (2022) 718, https://doi.org/10.3390/microorganisms10040718.
[55] P.M.R. Pereira, S. Silva, J.A.S. Cavaleiro, C.A.F. Ribeiro, J.P.C. Tomé, R. Fernandes, Galactodendritic phthalocyanine targets carbohydrate-binding proteins enhancing photodynamic therapy, PLoS One 9 (2014) e95529, https://doi.org/10.1371/journal.pone.0095529.
[56] A. Sułek, B. Pucelik, M. Kobielusz, A. Barzowska, J.M. Dąbrowski, Photodynamic inactivation of bacteria with porphyrin derivatives: effect of charge, lipophilicity, ROS generation, and cellular uptake on their biological activity in vitro, Int. J. Mol. Sci. 21 (2020) 8716, https://doi.org/10.3390/ijms21228716.
[57] M. Bispo, S. Suhani, J.M. van Dijl, Empowering antimicrobial photodynamic therapy of *Staphylococcus aureus* infections with potassium iodide, J. Photochem. Photobiol. B 225 (2021) 112334, https://doi.org/10.1016/j.jphotobiol.2021.112334.
[58] G.A. Pankey, L.D. Sabath, Clinical relevance of bacteriostatic versus bactericidal mechanisms of action in the treatment of gram-positive bacterial infections, Clin. Infect. Dis. 38 (2004) 864–870, https://doi.org/10.1086/381972.
[59] S. George, M.R. Hamblin, A. Kishen, Uptake pathways of anionic and cationic photosensitizers into bacteria, Photochem. Photobiol. Sci. 8 (2009) 788–795, https://doi.org/10.1039/b809624d.
[60] L.D. Costa, C. Vieira, S. Hackbarth, M.G.P.M.S. Neves, A. Almeida, M.A.F. Faustino, A.C. Tomé, Photodynamic inactivation of *Escherichia coli* and *Staphylococcus aureus* by cationic diketopyrrolopyrroles, Dyes Pigments 244 (2026) 113101, https://doi.org/10.1016/j.dyepig.2025.113101.
[61] C. Vieira, A.T.P.C. Gomes, M.Q. Mesquita, N.M.M. Moura, M.G.P.M.S. Neves, M.A. F. Faustino, A. Almeida, An insight into the potentiation effect of potassium iodide on aPDT efficacy, Front. Microbiol. 9 (2018), https://doi.org/10.3389/fmicb.2018.02665.
[62] C. Vieira, M. Bartolomeu, P.P. Gallego, M.G.P.M.S. Neves, J.L. Romalde, M.A. F. Faustino, A. Almeida, Photodynamic inactivation mediated by TMPyP and potassium iodide: a promising strategy for *Vibrio anguillarum* control in aquaculture, Dyes Pigments (2026) 113981, https://doi.org/10.1016/j.dyepig.2026.113981.
[63] F. Freire, C. Ferraresi, A.O.C. Jorge, M.R. Hamblin, Photodynamic therapy of oral Candida infection in a mouse model, J. Photochem. Photobiol. B 159 (2016) 161–168, https://doi.org/10.1016/j.jphotobiol.2016.03.049.
[64] M. Du, W. Xuan, X. Zhen, L. He, L. Lan, S. Yang, N. Wu, J. Qin, R. Zhao, J. Qin, J. Lan, H. Lu, C. Liang, Y. Li, M.R. Hamblin, L. Huang, Antimicrobial photodynamic therapy for oral Candida infection in adult AIDS patients: a pilot clinical trial, Photodiagn. Photodyn. Ther. 34 (2021) 102310, https://doi.org/10.1016/j.pdpdt.2021.102310.